parameter a in the form factors is expected to be related to the mass differences of the baryon levels.[16] We have not said anything about the mass spectrum in $O(4,2)$. This can be discussed with tensor operator methods or with the generalized Majorana equations. Also, the behavior of the mesons and decay properties are being investigated.

Finally, it should be remarked that in the present formalism the cross-channel amplitudes have to be evaluated separately because the boosters are different.[1,2]

[16] *Note added in proof.* Positive magnetic moments and correct mass spectra are obtained from a new current which contains besides Γ_μ a convective current P_μ, in a forthcoming paper by A. O. Barut, D. Corrigan, and H. Kleinert [Phys. Rev. (to be published)].

PHYSICAL REVIEW VOLUME 161, NUMBER 5 25 SEPTEMBER 1967

Poles and Resonances in η Photoproduction

S. R. DEANS AND WENDELL G. HOLLADAY
Department of Physics and Astronomy, Vanderbilt University, Nashville, Tennessee
(Received 17 April 1967)

Various combinations of poles and resonances have been tried to determine just which combinations yield reasonable fits to the total and differential cross-section data for the process $\gamma+p\rightarrow\eta+p$. In each case the best values of the parameters have been obtained by minimizing χ^2. Excellent fits ($\chi^2/N\approx0.8$) are obtained for certain combinations of poles and resonances. All solutions with the $S_{11}(1570)$ resonance omitted have rather poor values of χ^2, and the $P_{11}(1400)$ resonance cannot be used in lieu of the $S_{11}(1570)$ in this process. Evidence is obtained for classifying the $F_{15}(1688)$ as a member of an octet rather than a 27-plet. For all the models considered here, the value of the η-nucleon coupling constant ($g_\eta^2/4\pi$) is less than 2, indicating a D/F ratio larger than $\frac{3}{2}$.

I. INTRODUCTION

THE differential cross section for the process $\gamma+p\rightarrow\eta+p$ has recently been measured by three different groups. Prepost *et al.*[1] (Stanford) made a measurement of $d\sigma/d\Omega$ at approximately 100° (center of mass) from threshold (~710 MeV) to around 960-MeV lab photon energy. Bacci *et al.*[2,3] (Frascati) measured $d\sigma/d\Omega$ over an energy range of 800–1000 MeV and η center-of-mass angle of 106° to 120°. Heusch *et al.*[4] (Caltech) made measurements at 45° from 940 to 1090 MeV. Examination of the data from these experiments shows that there is a rather sharp rise in the cross section just above threshold with a peak being reached in the general vicinity of 1570-MeV total center-of-mass energy. Following the rapid rise there is an almost equally rapid drop between the peak and around 1670 MeV with a hint of another rise beginning around 1710 MeV. A similar structure is also observed in η production by pions on nucleons.[5]

Several authors[6,7] have analyzed the process $\pi^-+p\rightarrow\eta+n$. Better agreement with the experimental data has been found by those authors who use an S-wave resonance in the neighborhood of 1500 MeV. However, the work by Minami[8] indicates that the effects of the D_{13} resonance are comparable to or larger than those of the S_{11} resonance in the region of the peak. It has been pointed out by Heusch[9] that both in pion and photoproduction of eta particles the rise above threshold appears to have a positive second derivative which suggest a P-wave behavior. Thus, the S-wave can not fit both the threshold and the first few cross section points. According to Heusch,[9] Bloom and Prescott[10] have found that both S_{11} and P_{11} resonances will match the data.

A less extensive analysis of the η photoproduction data has been made. Along with the work of Bloom and Prescott mentioned above there is the work of Logan and Uchiyama-Campbell,[11] who found that an S wave gave a good fit to the total cross section. However, they did not use the Caltech data and, of course, the angular dependence of the Frascati data had no effect on their analysis. Minami[8] has studied the process $\gamma+p\rightarrow\eta+p$ in order to obtain information concerning the partial widths Γ_η and Γ_π of the S_{11} resonance. In his analysis

[1] R. Prepost, D. Lundquist, and D. Quinn, Phys. Rev. Letters **18**, 82 (1967).
[2] C. Bacci, G. Penso, G. Salvini, C. Mencuccini, and V. Silvestrini, Phys. Rev. Letters **16**, 157 (1966).
[3] C. Bacci, C. Mencuccini, G. Penso, G. Salvini, and V. Silvestrini, Nuovo Cimento **45**, 983 (1966).
[4] C. A. Heusch, C. Y. Prescott, E. D. Bloom, and L. S. Rochester, Phys. Rev. Letters **17**, 573 (1966).
[5] F. Bulos *et al.*, Phys. Rev. Letters **13**, 486 (1964); W. B. Richards *et al.*, *ibid.* **16**, 1221 (1966).
[6] F. Uchiyama-Campbell, Phys. Letters **18**, 189 (1965); A. W. Hendry and R. G. Moorhouse, *ibid.* **18**, 171 (1965); P. N. Dobson, Phys. Rev. **146**, 1022 (1965); F. Uchiyama-Campbell and R. K. Logan, *ibid.* **149**, 1220 (1966); G. Altarelli, F. Buccella, and R. Gatto, Nuovo Cimento **35**, 331 (1965).
[7] J. S. Ball, Phys. Rev. **149**, 1191 (1966).
[8] S. Minami, Phys. Rev. **147**, 1123 (1966).
[9] C. A. Heusch, lecture delivered at the International School of Physics "Ettore Majorana," Erice, Sicily, 1966 (unpublished).
[10] E. D. Bloom and C. Y. Prescott (unpublished).
[11] R. K. Logan and F. Uchiyama-Campbell, Phys. Rev. **153**, 1634 (1967).

only the Frascati data were used and no attempt was made toward a systematic fitting of all the data to various possible poles and resonances which may contribute to this process.

In view of the lack of any extensive fitting to the existing η photoproduction data we have tried various combinations of poles and resonances and have determined the parameters to minimize χ^2 in each case. We have used data below 1100 MeV for the laboratory photon energy or 1716 MeV in the center-of-mass system. The calculations which are presented in this paper are of the one-particle-exchange type (OPET), which in the broad sense involves poles and resonances in the direct channel as well as exchange terms, and are undertaken with precisely the same point of view as that adopted by Harun-ar-Rashid and Moravcsik[12] in their OPET treatment of pion photoproduction. It is our purpose to determine just which combinations yield reasonable fits, and to determine the best values of the parameters which enter into the calculations.

There have been models, which are in some respects similar to ours, proposed for the process $\gamma+p\rightarrow\eta+p$. They appeared prior to the recent experimental data and thus little or no analysis of data could be made. The resonance model proposed by Nishimura[13] is probably most closely related to ours; however, in that model the S_{11} and P_{11} resonances were not considered. The model of Minami and Moss[14] includes only the proton pole and D_{13} resonance and neglects the effect of the anomalous magnetic moment of the proton.

II. KINEMATICS

The kinematics for processes of the type considered here have been given by many authors. The notation used in this paper is similar to that used by Chew, Goldberger, Low, and Nambu,[15] hereafter referred to as CGLN, for pion photoproduction and Nishimura[13] for η photoproduction. We give a summary of the important results for the sake of completeness and to establish notation.

The four-momenta of the particles in the reaction $\gamma+N\rightarrow\eta+N$ are denoted by $k=(\mathbf{k},i\omega_1)$, $p_1=(\mathbf{p}_1,iE_1)$, $q=(\mathbf{q},i\omega_2)$, and $p_2=(\mathbf{p}_2,iE_2)$ for the photon, initial nucleon, η, and final nucleon, respectively. The nucleon mass is denoted by M and the η mass by m. We shall use a system of units where $\hbar=c=1$. The total center-of-mass energy W is related to the laboratory photon energy E_γ by

$$W^2=2ME_\gamma+M^2 \tag{2.1}$$

and the center-of-mass production angle Θ of the η is given by

$$\cos\Theta=\frac{\mathbf{k}\cdot\mathbf{q}}{|\mathbf{k}|\,|\mathbf{q}|}=x. \tag{2.2}$$

The invariants s, t, and u are defined by

$$s=-(p_1+k)^2, \tag{2.3a}$$

$$t=-(q-k)^2, \tag{2.3b}$$

$$u=-(p_1-q)^2. \tag{2.3c}$$

We decompose the S matrix in terms of the T matrix in the usual fashion:

$$S_{fi}=\frac{-i}{(2\pi)^2}\delta^{(4)}(k+p_1-q-p_2)\times\frac{M}{(4E_1E_2\omega_1\omega_2)^{1/2}}\bar{U}(p_2)TU(p_1), \tag{2.4}$$

where the Dirac spinors satisfy

$$\bar{U}(p_2)(i\gamma\cdot p_2+M)=0, \tag{2.5a}$$

$$(i\gamma\cdot p_1+M)U(p_1)=0. \tag{2.5b}$$

The T matrix of (2.4) can be expanded in terms of four Lorentz- and gauge-invariant operators:

$$T=\sum_{j=1}^{4}A_j(s,t,u)O_j, \tag{2.6}$$

where

$$O_1=i\gamma_5\gamma\cdot\epsilon\gamma\cdot k, \tag{2.7a}$$

$$O_2=2i\gamma_5(\epsilon\cdot Pq\cdot k-\epsilon\cdot qk\cdot P), \tag{2.7b}$$

$$O_3=\gamma_5(\gamma\cdot\epsilon q\cdot k-\gamma\cdot k\epsilon\cdot q), \tag{2.7c}$$

$$O_4=2\gamma_5(\gamma\cdot\epsilon k\cdot P-\gamma\cdot k\epsilon\cdot P-iM\gamma\cdot\epsilon\gamma\cdot k), \tag{2.7d}$$

and ϵ is the polarization vector of the photon. We have assumed odd η-nucleon parity and have defined $2P=p_1+p_2$. The A_j amplitudes (or $\mathcal{F}_i$ amplitudes defined below) are matrices in isospin space and can be decomposed into isoscalar A_j^S and isovector A_j^V parts by writing

$$A_j=A_j^S1+A_j^V\tau_3. \tag{2.8}$$

It will be convenient to write the A_j amplitudes in terms of the $\mathcal{F}_i$ amplitudes used by CGLN. The relation between the two sets of amplitudes is[13,16]

$$\mathcal{F}_i=\zeta_{ij}A_j, \tag{2.9}$$

where the matrix ζ can be obtained from Refs. 13 or 16.

III. POLE TERMS

The contribution made to the A_j amplitudes [and hence the $\mathcal{F}_i$ amplitudes through (2.9)] by the pole

[12] A. M. Harun-ar-Rashid and M. J. Moravcsik, Ann. Phys. (N. Y.) **35**, 331 (1965).
[13] K. Nishimura, Nuovo Cimento **29**, 1186 (1963).
[14] S. Minami and T. A. Moss, Phys. Rev. **132**, 838 (1963).
[15] G. F. Chew, M. L. Goldberger, F. E. Low, and Y. Nambu, Phys. Rev. **106**, 1345 (1957).
[16] S. Hatsukade and H. J. Schnitzer, Phys. Rev. **128**, 468 (1962).

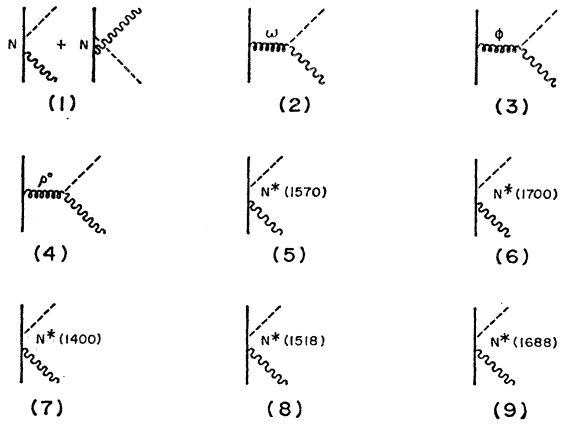

FIG. 1. Processes used in this calculation. The numbers are associated with the index λ.

terms in graphs (1) through (4) in Fig. 1 can be found by using Table I and the appropriate set of Feynman rules. (We have always used the sum of the contributions of the two graphs associated with $\lambda=1$ in Fig. 1 and therefore we carry only one index for the combination.) When one or more of the graphs with $\lambda=1$ through $\lambda=4$ is included we write the $A_j{}^\xi$ amplitude as the sum[12] (index λ) over the desired graphs

$$A_j{}^\xi=\sum_\lambda B_j{}^{\xi\lambda}X_{\xi\lambda}\,, \tag{3.1}$$

where ξ, an isospin index, is either S or V. X is a matrix which is dependent upon whether or not a given graph makes a contribution to the isoscalar or isovector part of the amplitude and is given in Table II. We have thus expanded A_j, through (2.8) and (3.1), in such a manner that the $B_j{}^{\xi\lambda}$ can be easily found by using Feynman rules. The $B_j{}^{\xi\lambda}$ are shown in Table III, where we have defined $\mu^S=(\mu_p+\mu_n)/2$ and $\mu^V=(\mu_p-\mu_n)/2$ with μ_p and μ_n representing the anomalous magnetic moments of the proton and neutron. Also, we have written $G_\nu{}^V=g_{\nu\gamma\eta}g_\nu{}^V$ and $G_\nu{}^T=g_{\nu\gamma\eta}g_\nu{}^T$, where ν represents the particle ω, ρ, or ϕ.

In making calculations we have neglected the width of the ω and ϕ mesons and have assumed that they give a true pole contribution in the t channel. The width of the ρ meson has been taken into account by modifying the denominator of the propagator.[17] In place of M_ρ we have written $M_\rho-i\Gamma_\rho/2$, where Γ_ρ is the width of the resonance.[18]

TABLE I. Vertex factors and propagators.[a]

Vertex or propagator	Vertex factor or propagator
ηNN	$ig_\eta\gamma_5$
γNN	$-ie\gamma\cdot\epsilon\dfrac{1+\tau_3}{2}+\gamma\cdot\epsilon\gamma\cdot k\left(\dfrac{\mu_p+\mu_n}{2}1+\dfrac{\mu_p-\mu_n}{2}\tau_3\right)$
Fermion propagator	$\dfrac{M-i\gamma\cdot P}{M^2+P^2}$
ωNN or ϕNN	$-ig_\omega{}^V\gamma_\mu+\dfrac{ig_\omega{}^T}{2M}\sigma_{\mu\nu}(p_2-p_1)_\nu\{\omega\to\phi$ for $\phi NN\}$
$\omega\gamma\eta$ or $\phi\gamma\eta$	$\dfrac{-ig_{\omega\gamma\eta}}{m'}\epsilon_{\sigma\kappa\lambda\xi}\epsilon_\kappa k_\lambda q_\xi\{\omega\to\phi$ for $\phi\gamma\eta\}$
ρNN	$-ig_\rho{}^V\gamma_\mu\tau_3+\dfrac{ig_\rho{}^T}{2M}\sigma_{\mu\nu}(p_2-p_1)_\nu\tau_3$
$\rho\gamma\eta$	$-i\dfrac{g_{\rho\gamma\eta}}{m'}\epsilon_{\sigma\kappa\lambda\xi}\epsilon_\kappa k_\lambda q_\xi$
Vector boson propagator	$\dfrac{\delta_{\sigma\mu}+[(k-q)_\sigma(k-q)_\mu/M_\omega{}^2]}{M_\omega{}^2-t}\begin{Bmatrix}\omega\to\phi$ for $\phi NN\\ \omega\to\rho$ for $\rho NN\end{Bmatrix}$.

[a] The mass m' is an arbitrary mass inserted to make the coupling constant dimensionless. It is taken to be 1 BeV in the calculations.

IV. RESONANCE TERMS

A multipole expansion of the $\mathcal{F}_i$ amplitudes has been given by CGLN [Eqs. (7.3)–(7.6)]. Using this expansion we find the contribution made to the $\mathcal{F}_i$ amplitudes by a given resonance. The resonance terms in the s channel that might contribute to the process $\gamma p\to\eta p$ are given in Table IV along with their contributions to the $\mathcal{F}_i$ amplitudes. The energy-dependent amplitudes $M_{l^\pm}$ and $E_{l^\pm}$ which appear in Table IV are given by the Breit-Wigner forms

TABLE II. The matrix elements $X_{\xi\lambda}$.

ξ \ λ	1	2	3	4
S	1	1	1	0
V	1	0	0	1

$$E_{l^\pm}=\frac{\frac{1}{2}}{[|\mathbf{q}|\,|\mathbf{k}|j_\gamma(j_\gamma+1)]^{1/2}}\frac{(\Gamma_{l^\pm}{}^E\Gamma_{l^\pm})^{1/2}}{(W_r-W)-i\Gamma/2} \tag{4.1}$$

and

$$M_{l^\pm}=\frac{\frac{1}{2}}{[|\mathbf{q}|\,|\mathbf{k}|j_\gamma(j_\gamma+1)]^{1/2}}\frac{(\Gamma_{l^\pm}{}^M\Gamma_{l^\pm})^{1/2}}{(W_r-W)-i\Gamma/2}\,, \tag{4.2}$$

where $j_\gamma=l+1$ for E_{l^+}, $j_\gamma=l-1$ for E_{l^-}, $j_\gamma=l$ for $M_{l^\pm}$ and l is the orbital angular momentum of the final state. The partial widths are given by Blatt and Weisskopf[19]; for example,

$$\Gamma_{l^\pm}=2|\mathbf{q}|Rv_l(|\mathbf{q}|R)\gamma_{l^\pm}\,, \tag{4.3}$$

where R is an interaction radius (taken to be about one fermi in the calculations), $v_l(|\mathbf{q}|R)$ is a barrier penetra-

[17] M. Parkinson, Phys. Rev. Letters **18**, 270 (1967).

[18] A. H. Rosenfeld, A. Barbaro-Galtieri, W. J. Podolsky, L. R. Price, P. Sodin, C. G. Wohl, M. Roos, and W. J. Willis, Rev. Mod. Phys. **39**, 1 (1967).

[19] J. M. Blatt and V. F. Weisskopf, *Theoretical Nuclear Physics* (John Wiley & Sons, Inc., New York, 1952).

TABLE III. The pole contributions to the $B_j{}^{\xi\lambda}$ amplitudes.

λ \ j	1	2	3	4
1	$\frac{1}{2}eg_\eta \dfrac{m^2-t}{(M^2-s)(M^2-u)}$	$\dfrac{eg_\eta}{(M^2-s)(M^2-u)}$	$\mu^\xi g_\eta \dfrac{s-u}{(M^2-s)(M^2-u)}$	$\mu^\xi g_\eta \dfrac{t-m^2}{(M^2-s)(M^2-u)}$
2 if $\nu=\omega$ 3 if $\nu=\phi$ 4 if $\nu=\rho$	$\dfrac{G_\nu{}^T t}{2m'M(t-M_\nu{}^2)}$	$\dfrac{G_\nu{}^T}{2m'M(M_\nu{}^2-t)}$	0	$\dfrac{G_\nu{}^V}{m'(M_\nu{}^2-t)}$

TABLE IV. The resonance contributions to the $\mathcal{F}_i$ amplitudes.

Resonance[a] Γ	Amplitude $\mathcal{F}_1$	$\mathcal{F}_2$	$\mathcal{F}_3$	$\mathcal{F}_4$
$S_{11}N^*(1570)$ 130	$E_0{}^+$	0	0	0
$S_{11}'N^*(1700)$ 240	$E'_0{}^+$	0	0	0
$P_{11}N^*(1400)$ 210	0	$M_1{}^-$	0	0
$D_{13}N^*(1518)$ 100	$3M_2{}^-+E_2{}^-$	$6M_2{}^-x$	0	$-3(M_2{}^-+E_2{}^-)$
$D_{15}N^*(1688)$ 100	$\frac{3}{2}(2M_2{}^++E_2{}^+)(5x^2-1)$	$9M_2{}^+x$	$15(E_2{}^+-M_2{}^+)x$	$3(M_2{}^+-E_2{}^+)$
$F_{15}N^*(1688)$ 100	$(12M_3{}^-+3E_3{}^-)x$	$\frac{3}{2}M_3{}^-(5x^2-1)$	$3(M_3{}^-+E_3{}^-)$	$-15(M_3{}^-+E_3{}^-)x$

[a] Reference 18.

tion factor also tabulated by Blatt and Weisskopf and γ_l is a reduced width which is unknown. The reduced widths $\gamma_l{}^\pm$, $\gamma_l{}^{\pm E}$, and $\gamma_l{}^{\pm M}$ always appear as products $\gamma_l{}^\pm\gamma_l{}^{\pm E}$ or $\gamma_l{}^\pm\gamma_l{}^{\pm M}$ in a resonance formula. Since we do not know either term in the product we choose these products as the adjustable parameters and rewrite them as $(\gamma_l{}^\pm\gamma_l{}^{\pm E})^{1/2}=\gamma^E(L_{2T2J})$, and $(\gamma_l{}^\pm\gamma_l{}^{\pm M})^{1/2}=\gamma^M(L_{2T2J})$. These parameters appear in Table V. Upon simplification the above equations can be written as indicated in Table V, where we have defined

$$Z=\frac{1}{(W_r-W)-i\Gamma/2}. \tag{4.4}$$

The total width Γ is approximated by that of the elastic width

$$\Gamma=\frac{|\mathbf{k}|}{|\mathbf{k}_r|}\frac{v_l(|\mathbf{k}|R)}{v_l(|\mathbf{k}_r|R)}\Gamma_r. \tag{4.5}$$

In all of these expressions the subscript r means evaluated at the resonance energy W_r. The values used for W_r and Γ_r are listed in Table IV.[18]

V. DIFFERENTIAL CROSS SECTION AND POLARIZATION

The differential cross section for unpolarized initial particles is given by[12,20]

$$\frac{d\sigma}{d\Omega}=\frac{|\mathbf{q}|}{|\mathbf{k}|}\Big\{|\mathcal{F}_1|^2+|\mathcal{F}_2|^2-2x\,\mathrm{Re}(\mathcal{F}_1{}^*\mathcal{F}_2)+\frac{1-x^2}{2}[|\mathcal{F}_3|^2+|\mathcal{F}_4|^2+2\,\mathrm{Re}(\mathcal{F}_1{}^*\mathcal{F}_4)+2\,\mathrm{Re}(\mathcal{F}_2{}^*\mathcal{F}_3)+2x\,\mathrm{Re}(\mathcal{F}_3{}^*\mathcal{F}_4)]\Big\}, \tag{5.1}$$

and the final proton polarization $\mathcal{P}$ in the direction of $\hat{k}\times\hat{q}$ is given by [12,20]

$$\mathcal{P}\frac{d\sigma}{d\Omega}=\frac{|\mathbf{q}|}{|\mathbf{k}|}\sin\Theta\,\mathrm{Im}\{-2\mathcal{F}_1{}^*\mathcal{F}_2-\mathcal{F}_1{}^*\mathcal{F}_3+\mathcal{F}_2{}^*\mathcal{F}_4+\sin^2\Theta\mathcal{F}_3{}^*\mathcal{F}_4+\cos\Theta(\mathcal{F}_2{}^*\mathcal{F}_3-\mathcal{F}_1{}^*\mathcal{F}_4)\}. \tag{5.2}$$

The total $\mathcal{F}_i$ amplitudes for the process $\gamma+p\to\eta+p$ which appears in (5.1) and (5.2) are obtained by adding the resonance contribution to the pole contribution.

VI. ANALYSIS OF DATA

We have used the data from Refs. 1–4, omitting the earlier Frascati data[21,22] in favor of the more recent

TABLE V. The multipole amplitudes.

l \ Amplitude	E_{l+}	E_{l-}
0	$RZ\gamma^E(S_{11})/\sqrt{2}$	
1		
2	$\frac{RZ}{\sqrt{12}}\gamma^E(D_{15})[v_2(\|\mathbf{q}\|R)v_2(\|\mathbf{k}\|R)]^{1/2}$	$\frac{RZ}{\sqrt{2}}\gamma^E(D_{13})[v_2(\|\mathbf{q}\|R)]^{1/2}$
3		$\frac{RZ}{\sqrt{6}}\gamma^E(F_{15})[v_3(\|\mathbf{q}\|R)v_1(\|\mathbf{k}\|R)]^{1/2}$
l	M_{l+}	M_{l-}
0		
1		$\frac{RZ}{\sqrt{2}}\gamma^M(P_{11})[v_1(\|\mathbf{q}\|R)v_1(\|\mathbf{k}\|R)]^{1/2}$
2	$\frac{RZ}{\sqrt{6}}\gamma^M(D_{15})[v_2(\|\mathbf{q}\|R)v_2(\|\mathbf{k}\|R)]^{1/2}$	$\frac{RZ}{\sqrt{6}}\gamma^M(D_{13})[v_2(\|\mathbf{q}\|R)v_2(\|\mathbf{k}\|R)]^{1/2}$
3		$\frac{RZ}{\sqrt{12}}\gamma^M(F_{15})[v_3(\|\mathbf{q}\|R)v_3(\|\mathbf{k}\|R)]^{1/2}$

[20] M. J. Moravcsik, Phys. Rev. 125, 1088 (1962).

[21] C. Bacci, G. Penso, G. Salvini, and A. Wattenberg, Phys. Rev. Letters 11, 37 (1963).

[22] B. Delcourt, J. Lefrancois, J. P. Perez Y Jorba, and J. K. Walker, Phys. Letters 7, 215 (1963).

TABLE VI. Values of the parameters for various combinations of poles and resonance. The upper entry corresponds to the 0.31 branching ratio and the lower one to the 0.38 ratio.

Sol.	Poles and resonances	$g_\eta/(4\pi)^{1/2}$	$G_v{}^V/4\pi$	$G_v{}^T/4\pi$	$\gamma^E(S_{11})$	$\gamma^E(S_{11}')$	$\gamma^E(D_{13})$	$\gamma^M(D_{13})$	$\gamma^E(F_{15})$	$\gamma^M(F_{15})$	χ^2	χ^2/N
I	p	1.376									234.7	5.46
		1.264									241.5	5.62
II	S_{11}				−1.165						200.4	4.66
					−1.063						217.8	5.07
III	p, S_{11}	0.744			−1.286						65.7	1.56
		0.793			−1.182						51.7	1.23
IV	p, S_{11}, S_{11}'	0.839			−1.136	−0.236					57.7	1.41
		0.852			−1.066	−0.175					45.0	1.10
V	p, ω, S_{11}	1.319	0.121	0.074	−1.100						53.2	1.33
		1.378	0.103	0.132	−1.016						37.4	0.94
VI	p, ϕ, S_{11}	1.327	0.185	0.087	−1.112						53.2	1.33
		1.344	0.164	0.152	−1.014						37.2	0.93
VII	p, ρ, S_{11}	1.407	0.117	0.132	−1.140						54.3	1.36
		1.403	0.093	0.175	−1.073						37.7	0.94
VIII	p, S_{11}, F_{15}	0.873			−1.200				−0.521	0.164	47.0	1.17
		0.992			−1.061				−0.270	−0.380	33.9	0.85
IX	$p, \omega, S_{11}, F_{15}$	0.873	0.000	0.000	−1.200				−0.521	0.164	47.0	1.24
		1.031	0.028	0.000	−1.061				−0.220	−0.405	33.6	0.88
X	$p, \omega, S_{11}, F_{15}$	1.319	0.115	0.088	−1.100				−0.261	−0.015	51.0	1.34
		1.378	0.091	0.139	−1.016				−0.106	−0.248	34.6	0.91
XI	p, D_{13}, S_{11}	1.157			−0.981		−0.734	−0.024			59.0	1.47
		1.015			−0.981		−0.647	−0.546			41.1	1.03

results over essentially the same energy range. There are, in all, 44 energy- and angle-dependent differential cross section points. We have fitted these points to various poles and resonances in order to see just which combinations are needed to describe accurately the data. In Table VI we show some of the combinations tried. In each case we allowed the parameters to vary and minimized χ^2. However, it is quite possible in many cases that one might find an entirely different set of values for the parameters with only a slightly changed value of χ^2. No change results in χ^2 if all parameters undergo a simultaneous change of sign since $d\sigma/d\Omega$ is even under this interchange. (The polarization is also unaltered by replacing all parameters by their negative.)

In view of the uncertainty[7,11] in the branching ratio

$$\frac{\eta \rightarrow \gamma\gamma}{\eta \rightarrow \text{all modes}}$$

we have used the extreme values of 0.31[18] and 0.38.[2–4] The Frascati and Caltech results are dependent upon this ratio while the Stanford data are not. The upper entry in Table VI corresponds to the 0.31 branching ratio while the lower entry corresponds to the 0.38 ratio. All figures are drawn using the 0.38 ratio. One will notice immediately that the better solutions tend to have larger values of χ^2 for the 0.31 branching ratio. This is not difficult to understand since the overlapping Frascati and Stanford data are separated to a greater extent for the 0.31 value of the ratio than for the 0.38 value. However, the smaller value of the ratio leads to longer error bars, which, for the poorer solutions (I and II), have more effect than the separation of the data on the χ^2 values, which therefore become smaller. Unless otherwise stated, the comments in the following section will refer to the 0.38 ratio although the general over-all conclusions apply in either case, the main difference being the values of χ^2.

VII. DISCUSSION AND CONCLUSIONS

We shall, for convenience, refer to the various rows of Table VI as Sol. I, Sol. II, etc. The curves which appear in Figs. 2–8 are designated in the same fashion. The data points in these figures are coded as follows. The open circles represent the Stanford data[1]; the solid circles, the Frascati data[2,3]; and the solid triangles, the Caltech data.[4]

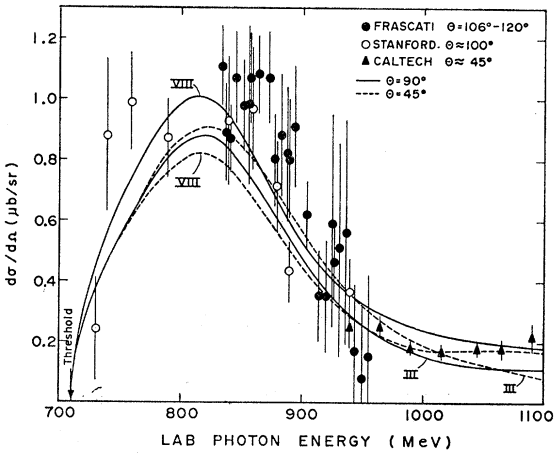

FIG. 2. Differential cross section curves for Sol. III and Sol. VIII (see Table VI) as a function of energy for $\Theta=90°$ and $\Theta=45°$. The experimental points are over the indicated range of angles.

We find that one graph (a single value of λ from Fig. 1) is not sufficient to describe the experimental results. Our results for $\lambda=1$ and for $\lambda=5$ are shown as Sol. I and Sol. II, respectively. If we omit the Caltech data as did Logan and Uchiyama-Campbell[11] we obtain a fit for the S_{11} which is not unlike theirs. The results, not shown, obtained for vector meson exchange ($\lambda=4$, for example) are worse than Sol. I. A very definite improvement is noted when the proton pole and the S_{11} resonance are put in together. The value of χ^2/N drops to 1.23, which is not bad considering the simplicity of the model. (N is the number of data points minus the number of varied parameters.) There are various ways to improve the fit obtained in Sol. III, the simplest of which is to include a vector meson or add another resonance.

The vector-meson exchange, Sols. V–VII, has the effect of causing the η-nucleon coupling constant

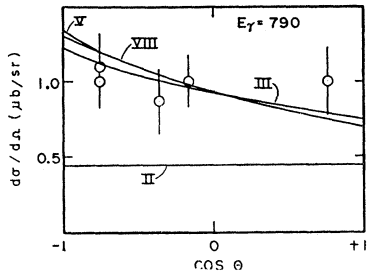

FIG. 3. The differential cross section as a function of cosΘ at $E_\gamma=790$ MeV. The curves in this and subsequent figures are labeled by Roman numerals which refer to Table VI.

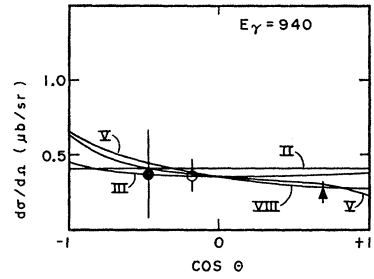

FIG. 4. The differential cross section as a function of cosΘ at $E_\gamma=940$ MeV.

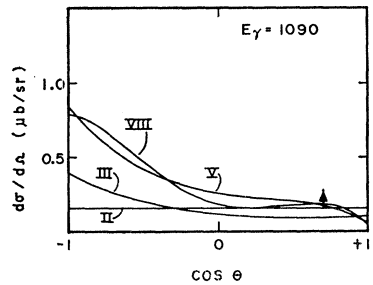

FIG. 5. The differential cross section as a function of cosΘ at $E_\gamma=1090$ MeV.

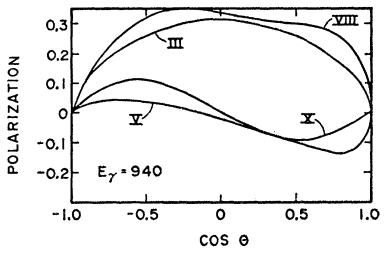

FIG. 6. Polarization in the direction $\mathbf{k}\times\mathbf{q}$ as a function of cosΘ at $E_\gamma=940$ MeV.

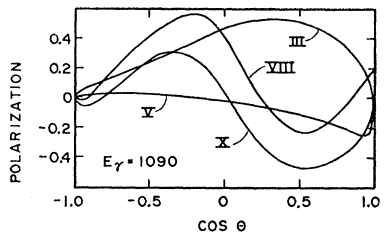

FIG. 7. Polarization in the direction $\mathbf{k}\times\mathbf{q}$ as a function of cosΘ at $E_\gamma=1090$ MeV.

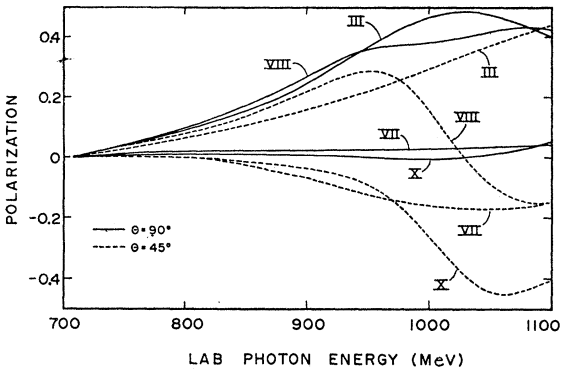

FIG. 8. Polarization in the direction $\mathbf{k}\times\mathbf{q}$ as a function of energy for $\Theta=90°$ and $\Theta=45°$.

$g_\eta/(4\pi)^{1/2}$ to rise to a value consistent with a D/F ratio[23] of about $\frac{3}{2}$. This value, $g_\eta^2/4\pi\approx1.8$, is very close to the exact and broken SU_{6W} prediction of 1.73.[24] As might be expected, very little improvement is found by trying more than one exchanged vector meson. Other resonances that can be added to the proton pole and the S_{11} resonance are the $S_{11}'\equiv S_{11}(1700)$, P_{11}, D_{13}, D_{15}, and F_{15} resonances. Of these possibilities we find that the F_{15} resonance yields the best fit in the sense of least χ^2/N (Sol. VIII). We show two other possibilities for comparison (Sols. IV and XI). It is clear from Sols. VIII and IX that based on the presently available data there is really no compelling reason to include a vector-meson exchange. The χ^2 values for all solutions would drop by

[23] P. A. Carruthers, *Introduction to Unitary Symmetry* (Interscience Publishers, Inc., New York, 1966).
[24] S. N. Gupta, Phys. Rev. **151**, 1235 (1966).

TABLE VII. Separate contributions to the differential cross section for $E_\gamma = 1047$ MeV and $\Theta = 45°$.

	$d\sigma/d\Omega$ (F_{15} only) (μb/sr)	$d\sigma/d\Omega$ (other) (μb/sr)	$d\sigma/d\Omega$ (interference) (μb/sr)	$d\sigma/d\Omega$ (total) (μb/sr)
Fixed F_{15} contribution, $\gamma^E(F_{15}) = -2.0$; $\gamma^M(F_{15}) = 0$	2.08	0.71	−2.09	0.70
Fixed F_{15} contribution, $\gamma^E(F_{15}) = 0$; $\gamma^M(F_{15}) = -3.2$	1.91	1.15	−2.46	0.60
Sol. VIII	0.080	0.093	+0.004	0.177

more than 4 if we omitted the 890-MeV Stanford point[11] which is displaced somewhat with respect to other points that are close by. (This corresponds to $\chi^2/N \approx 0.8$ for the better fits.) There are at least two (probably more) reasonably good solutions for p, ω, S_{11}, and F_{15} which we show in Sol. IX and Sol. X. Clearly there is very little difference between Sol. VIII and Sol. IX. In Fig. 2 we show the differential cross section as a function of energy at two angles for Sol. III and Sol. VIII. With the exception of the first two all other solutions shown in Table VI have similar curves.[25] In Figs. 3–5 we show the differential cross section as a function of angle at $E_\gamma = 790$, 940, and 1090 MeV for the indicated solutions.

We tried the combination p, $P_{11}(1400)$ and p, $P_{11}(1512)$ and found rather poor χ^2 values ($\chi^2/N > 5$), indicating that the P_{11} cannot be used in lieu of the S_{11} in this provess. The best fit obtained with the S_{11} omitted involved p, ω, P_{11}, D_{13}, D_{15}, and F_{15} with a χ^2/N larger than 2. We therefore find, using the parameters of the relevant particles and resonant states in Ref. 18, that it is not possible to obtain an acceptable fit to the data without including the S_{11} resonance.

When the S_{11} is included it appears that the parameter $\gamma^E(S_{11})$ can be chosen to be approximately -1 in all cases. Our work suggests that perhaps the η-nucleon coupling constant should satisfy the inequality

$$g_\eta^2/4\pi < 2.0. \tag{7.1}$$

Evidence is obtained for not classifying the F_{15} as a member of a 27-plet by assuming that it is a member and examing the consequences of the assumption. If the F_{15} is a member of a **27** then we expect that it should contribute approximately 2 μb/sr to the differential cross section at $E_\gamma = 1047$ MeV and $\Theta = 45°$.[9,26,27] For this energy and angle it is possible to obtain $d\sigma/d\Omega \approx 2\mu$b/sr by choosing $\gamma^E(F_{15}) \approx -2$ or $\gamma^M(F_{15}) \approx -3.2$ and all other parameters zero. As can be seen from the Caltech data, $d\sigma/d\Omega$ is only one tenth of this value. We wish to know whether or not it is possible for interference effects to come into play in such a way as to reduce $d\sigma/d\Omega$ from 2μb/sr to 0.2 μb/sr when other parameters are allowed to vary and $\gamma^E(F_{15})$ is fixed at -2 or $\gamma^M(F_{15})$ is fixed at -3.2. We minimize χ^2 using only the Caltech data so as to try to force $d\sigma/d\Omega$ down to 0.2 μb/sr. After finding the minimum we break the differential cross section into three parts:

$$\frac{d\sigma}{d\Omega} = \frac{d\sigma}{d\Omega}(F_{15}\text{ only}) + \frac{d\sigma}{d\Omega}(\text{other}) + \frac{d\sigma}{d\Omega}(\text{interference}), \tag{7.2}$$

and calculate the three parts separately. In Table VII we show the results of this calculation.[28] For comparison we also show the same calcultaion for Sol. VIII where the fit was good. We conclude that interference effects are not strong enough to cause the required lowering. Thus assuming that the F_{15} belongs to a **27** leads to some unobserved predictions.

The contribution to $d\sigma/d\Omega$ made by the F_{15} in our solutions is consistent with an assignment of F_{15} to an octet. This consistency with an octet assignment was established in Ref. 26 under the assumption that the above-mentioned interference effects were sufficiently small which we find to be the case.

One would like to be able to eliminate as many solutions as possible. In this way more insight could be gained as to just which poles and resonances are making major contributions to this process. Such an elimination may not be possible on the basis of differential cross-section data alone; however, measurements in the backward direction around $E_\gamma = 1090$ MeV would be useful. (See Fig. 5.) Perhaps by a polarization measurement one would be able to eliminate many of the solutions which are shown in Table VI as well as some not shown which involve different resonance combinations. For example, a polarization measurement around $\Theta = 30°$ at two energies ($E_\gamma = 940$ and $E_\gamma = 1090$) would be enlightening as can be seen by examination of Figs. 6 and Fig. 7. Some of the solutions have quite different polarization curves as a function of energy, which we show in Fig. 8. Thus, aside from the apparent need for the S_{11} resonance, it appears that we need more experimental results before we know just which poles and resonances are making the major contributions to the process $\gamma + p \to \eta + p$.

[25] Care should be exercised in comparing the data in Fig. 2 with the curves, since each curve is drawn for a fixed angle and data were taken at different angles.

[26] C. A. Heusch, C. Y. Prescott, and R. F. Dashen, Phys. Rev. Letters **17**, 1019 (1966).

[27] R. F. Dashen, Nuovo Cimento **32**, 469 (1964).

[28] Various mixtures of $\gamma^E(F_{15})$ and $\gamma^M(F_{15})$ can be found which yield $d\sigma/d\Omega \approx 2\mu$b/sr, for example $\gamma^E(F_{15}) = \gamma^M(F_{15}) = -1.5$; however, the interference effects have been calculated for a number of possible mixtures and are found to be about the same as those shown in Table VII.